

**Ulrich L. Rohde**  
**Ajay K. Poddar**  
**Matthias Rudolph**

## **Transistor Applications from RF to Microwave Frequencies**

Theory of SiGe heterojunction bipolar transistor (HBT) Transistors and high-electron-mobility transistor (pHEMT) and practical circuits

From VHF to EHF Frequencies

### ***Example of a Microwave Oscillator design***

Oscillator Design is an autonomous problem in which there is no external driving source. This complicates the design process considerably, as the frequency of an oscillator is then an additional degree of freedom in the circuit that must be accounted for.

## The Spice Version Oscillator first

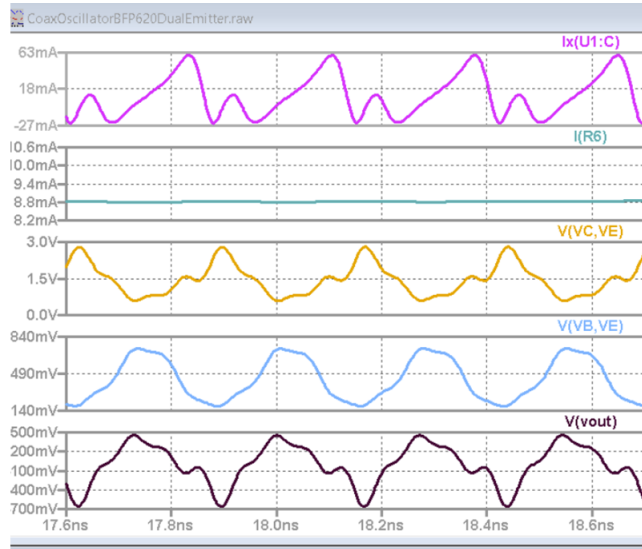
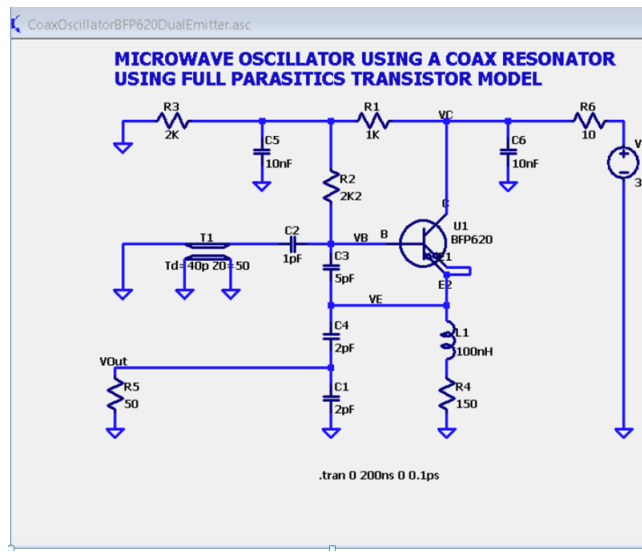


Figure 1: Microwave Oscillator Using a COAX Resonator Using Full Parasitics Transistor Model

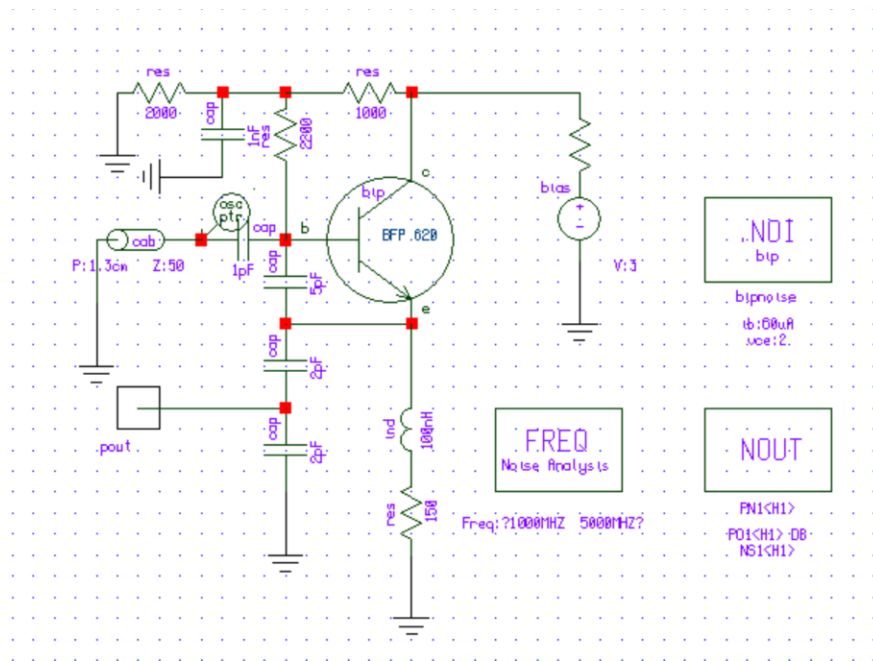


Figure 2a: Microwave Oscillator Using a COAX Resonator CAD Simulation Circuit

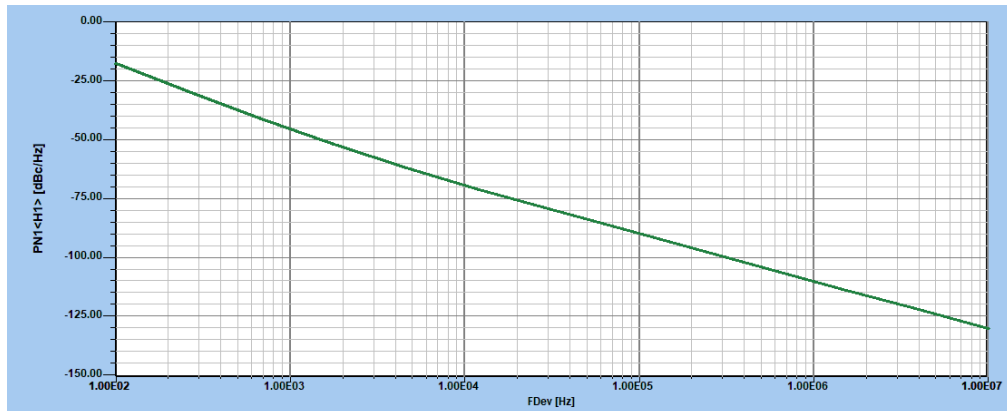


Figure 2b: Microwave Oscillator Using a COAX Resonator CAD Simulation Circuit – Simulated Phase Noise

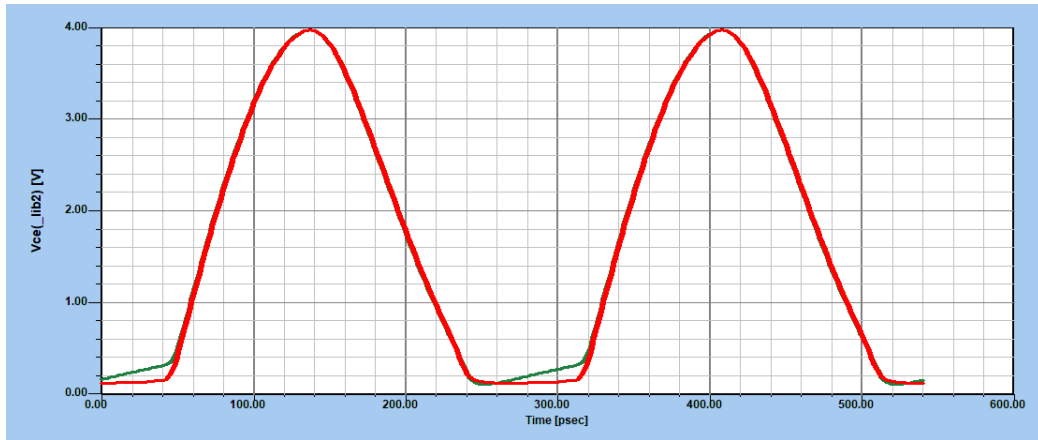


Figure 2c: Microwave Oscillator Using a COAX Resonator CAD Simulation Circuit – Simulated  $V_{CE}$

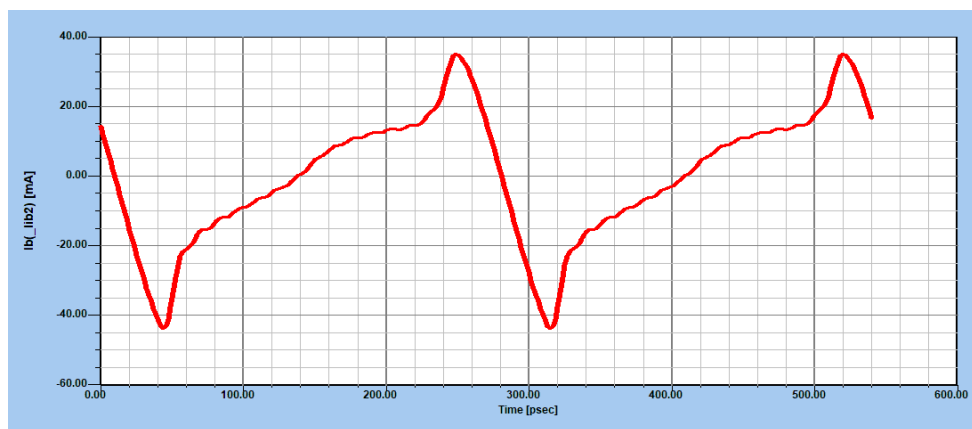
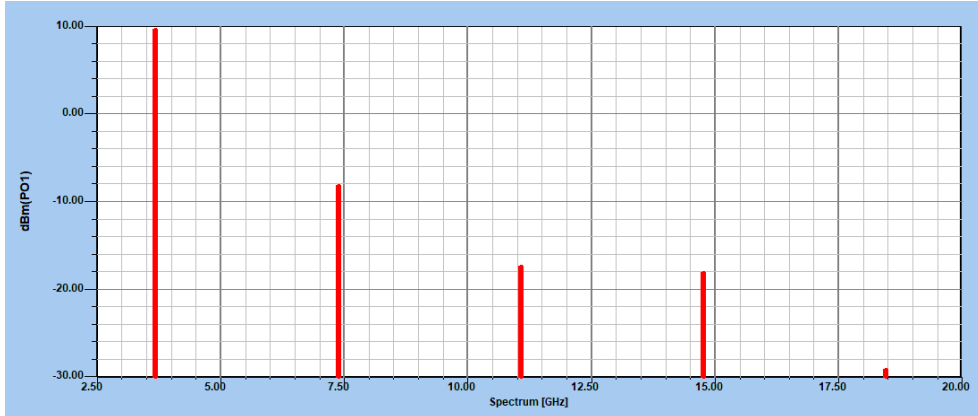


Figure 2d: Microwave Oscillator Using a COAX Resonator CAD Simulation Circuit – Simulated  $I_b$



Figure 2e: Microwave Oscillator Using a COAX Resonator CAD Simulation Circuit – Simulated  $I_c$



**Figure 2f: Microwave Oscillator Using a COAX Resonator CAD Simulation Circuit – Simulated  $P_{out}$  (dBm)**

### Introduction of the Harmonic Balance Method and non-linear noise calculation

There are now nonlinear Microwave CAD packages using the harmonic balance technique. Because of its nonlinear optimization capabilities, it is uniquely suited to the task of oscillator design [3]-[ 5]. The harmonic balance method seeks a solution to a steady-state nonlinear design problem by iteratively solving for a set of variables, referred to as state variables. The state variables can typically be chosen as the voltages at the linear–nonlinear interface in a circuit partitioned into linear and nonlinear segments. They are expressed as the phasor components, and their harmonics, of a sinusoidal excitation frequency. The state variables are usually found iteratively by a gradient-based technique which seeks a simultaneous solution for Kirchhoff's equations applied to the linear and nonlinear sides of the network separately [6]-[10].

For the non-autonomous, or driven, circuit, the driving frequency is known a priori and Kirchhoff's equations are a well-determined system of equations in which the phase and amplitude of the excitation appear on one side of the equations as forcing terms. In an autonomous circuit, the only excitation terms appearing in Kirchhoff's equations are DC sources. One stable solution to these equations for a circuit with no applied RF drive will always be the DC (or degenerate) solution, as all phasor terms at an arbitrarily chosen frequency can be set to zero and still satisfy the RF driving conditions (of zero excitation). For an autonomous circuit to have a solution to Kirchhoff's equations at nonzero frequencies, at least one additional degree of freedom is required, as there is one additional unknown in the equations – the oscillation frequency.

For oscillator analysis purposes (i.e. for a fixed circuit topology), the additional free parameter is just the unknown frequency of oscillation. For oscillator design purposes, the frequency is fixed as a design goal, and the required degree of freedom must be represented by a free circuit variable, such as a bias voltage or other tuning element. In this way, a solution can be found to the conditions for oscillation (which are just Kirchhoff's equations) by varying some circuit parameter. This parameter must be adjusted so that the equations can be satisfied at the oscillation frequency, with some set of (solution) state variables, which are determined at the same time.

The harmonic balance problem must then allow for the simultaneous solution of both the state variables and the circuit elements to satisfy Kirchhoff's equations under the chosen conditions (i.e. at the design frequency). In fact, these programs allow the user to set additional circuit parameters to be variables in order to optimize for other circuit responses, such as output power, efficiency, spectral purity, or distortion, while simultaneously satisfying Kirchhoff's equations. Consequently, the methodology of introducing additional degrees of freedom into the harmonic balance problem allows not only for the solution of autonomous designs but also for the optimization of all types of circuits for desired response.

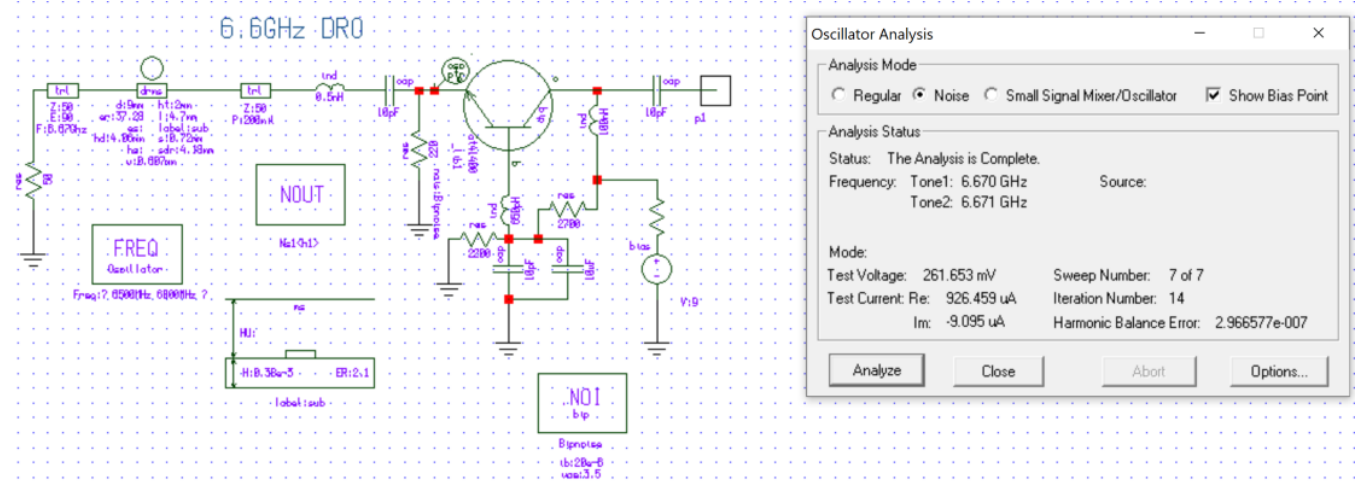


Figure 3a: DRO design example. ([9] [11])

As an example, above, we show a DRO design using a bipolar transistor embedded in a simple microstrip circuit. The specified optimization goals were 20 mW output power, at a frequency of 5 GHz. In the design, the additional degrees of freedom for the optimization problem and the oscillator synthesis were provided by the resonator diameter and the microstrip lengths together with the FET bias voltages.

Prior to circuit optimization, the program automatically optimizes the DRO dimensions to resonate at the  $TE_{01g}$  mode at 6.6 GHz. The pre-optimization is needed to ensure that the initial starting point for the design equations is within the operating regime. A sequence of optimizations was then performed by increasing the lower bounds on the output power. The maximum power available was found to be 6dBm with an efficiency of 3.28% but optimized for phase noise -112dBc/Hz indicates a high Q and low phase noise design. The bias point was  $V_D = 5.9$  V,  $I_b = 0.138mA$ , and  $I_c = 13.6$  mA. Output harmonics were about 24 dB below the fundamental.

The circuit can also be tuned by moving the metal tuning plate over the resonator. To tune to a frequency of 6.05 GHz, the circuit must be re-optimized with the plate distance  $s$  as the only tuning variable. This change to the single circuit parameter is needed to allow there to be a solution to Kirchhoff's equations at the new oscillation frequency. The values of the state variables are, of course, also different at the new point, and the output power is reduced correspondingly.

Bias Point Values	
Voltage	Current
$V_p() = 3.05824$ V	$I_p() = 0$ A
$V_{be1\_lib1} = 0.809963$ V	$I_{b\_lib1} = 0.138747$ mA
$V_{ce1\_lib1} = 5.93685$ V	$I_{c\_lib1} = 13.7624$ mA

Figure 3b: Bias Point Values

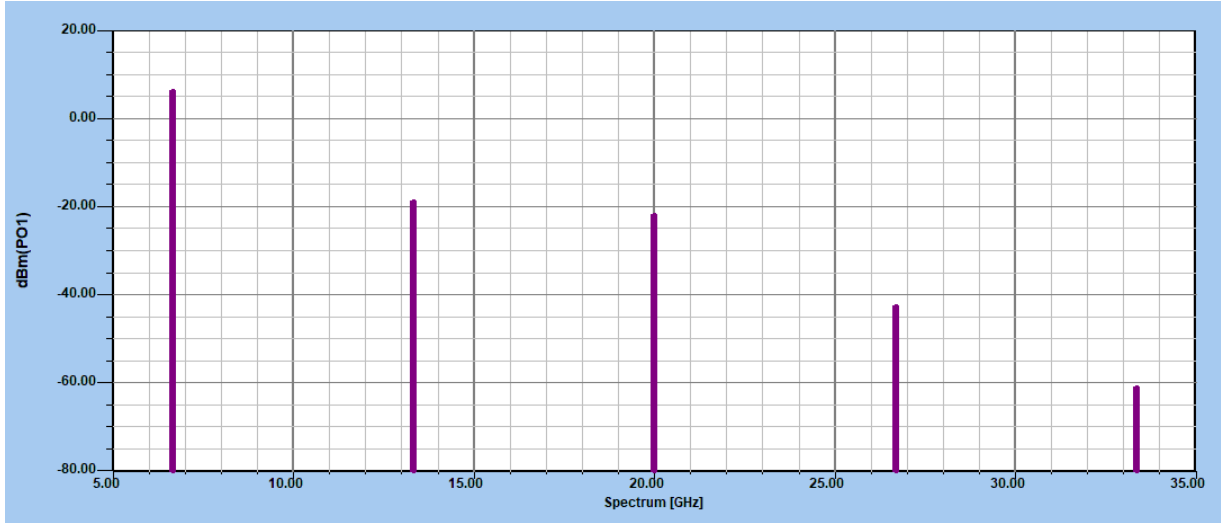


Figure 3c: 5GHz DRO design example - Simulated  $P_{out}$  (dBm) ([9] [Rizzoli et al. [11]])

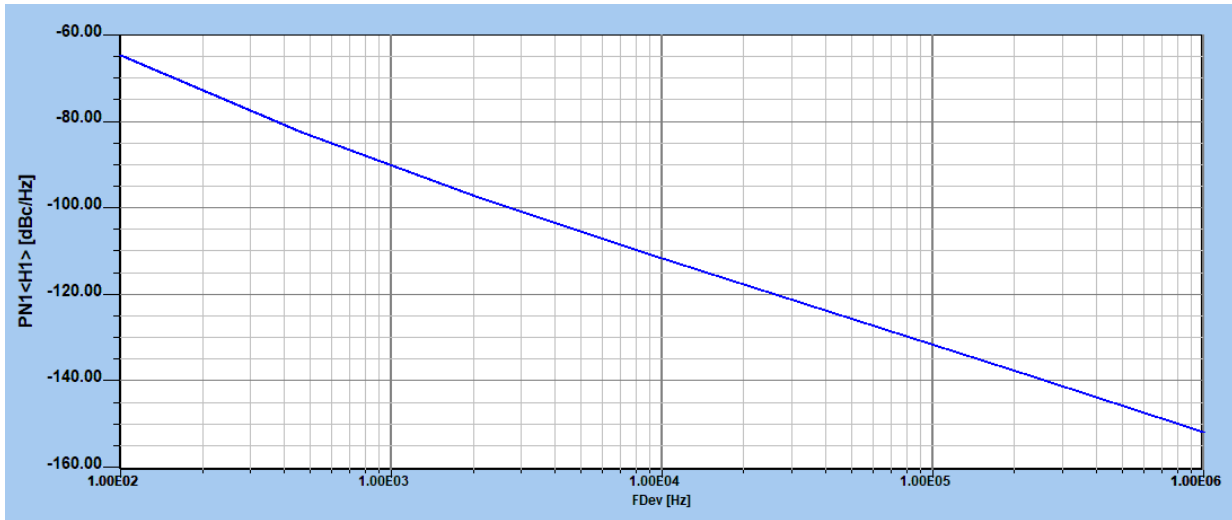


Figure 3d: 5GHz DRO design example (Ref [9] [Rizzoli et al. [11]])

As oscillator analysis can be performed by repetitively reoptimizing the tuning parameter ‘ $s$ ’ at a series of frequencies in the program and constructing a tuning curve of oscillation frequency versus  $s$ . For an oscillator of unknown frequency, the actual oscillation frequency can be determined by entering the tuning curve at the known value of  $s$ . Note that in the case of an oscillator analysis only a single tuning variable is adjusted at each frequency point, so that a tuning curve can be constructed to give a single, unique relationship between the design frequency and the actual circuit parameter value in the circuit being analyzed.

Although the harmonic balance approach ensures that a steady-state solution exists, the buildup of oscillations and the stability of the steady-state operating point also need to be addressed. One way to provide a numerical solution to this problem is to use the principles of bifurcation theory [9] [12]. Using the frequency of oscillation as a continuation parameter [13] and choosing the output power as a parameter to describe the circuit state, a solution path may be built by stepping the frequency through a prescribed range.

In summary, the advent of nonlinear CAD programs now allows the designer to verify many aspects of circuit operation not previously obtainable through linear programs alone. In this way, the levels of output power, harmonic content, DC-to-RF efficiency, device currents, and load pushing and pulling can be examined before the oscillator is constructed.

Next some more explanations about the non-linear program will follow

## Regular Analysis with the Harmonic Balance Program

### Formation of the Harmonic Balance Equations

Harmonic balance analysis consists of determining the periodic steady-state response of a fixed circuit given a pre-determined set of fundamental tones [1] [2]. The analysis is limited to periodic responses because the basis set, chosen to represent the physical signals in the circuit, are sinusoids, which are periodic. The Fourier series is used to represent these signals. In the single-tone case, a signal is given by

$$x(t) = \sum_{k=-NH}^{NH} X_k e^{jk\omega_0 t} \quad (1)$$

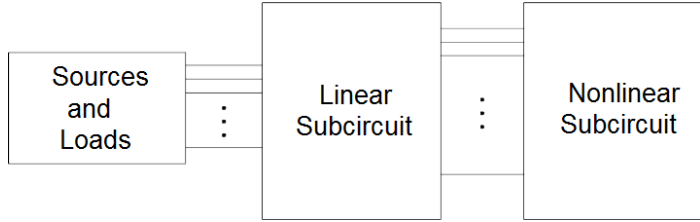


Figure 4: Separation of the linear and nonlinear subcircuits

where  $X_k = X_{-k}^*$ ,  $\omega_0$  is the fundamental frequency and NH is the number of harmonics chosen to represent the signal.

In harmonic balance, the circuit is usually divided into two subcircuits connected by wires forming multiport. One subcircuit contains the linear components of the circuit and the other contains the nonlinear device models as shown in Figure 4. The linear subcircuit response is calculated in the frequency domain at each harmonic component ( $k*\omega_0$ ) and is represented by a multiport Y matrix. This is the function performed by linear analysis.

The nonlinear subcircuit contains the active devices whose models compute the voltages and currents at the intrinsic ports of the device (parasitic elements are linear and absorbed by the linear subnetwork). The port voltages ( $v$ ) and currents ( $i$ ) are analytic or numeric functions of the device state variables ( $x$ ). Often the state variables represent physical voltages such as diode junction voltage or FET gate voltage, but are not restricted to physical quantities. The port voltages and currents are often functions of the time derivatives of the state variables (when a nonlinear capacitor is involved) and of time-delayed state variables (such as a time-delayed current source). Generally, the nonlinear device equations are of the form:

$$v(t) = \Phi \left[ x(t), \frac{dx}{dt}, \dots, \frac{d^n x}{dt^n}, x(t - \tau) \right] \quad (2)$$

$$i(t) = \Psi \left[ x(t), \frac{dx}{dt}, \dots, \frac{d^n x}{dt^n}, x(t - \tau) \right] \quad (3)$$

The device state variables, port voltages, and currents are transformed to the frequency domain using the discrete Fourier transforms as  $\mathbf{X}$ ,  $\mathbf{V}_k(\mathbf{X})$  and  $\mathbf{I}_k(\mathbf{X})$ , respectively. Kirchhoff's current law is applied to the interface between the subcircuits at each harmonic frequency:

$$\mathbf{Y}_k \mathbf{V}_k(\mathbf{X}) + \mathbf{I}_k(\mathbf{X}) + \mathbf{J}_k = 0 \quad (4)$$

where  $\mathbf{J}_k$  are the Norton equivalents of the applied generators. This constitutes the harmonic balance equations at each harmonic frequency. The object of the analysis is to find the set of state variables,  $\mathbf{X}$ , to satisfy equation (4).

When the analysis begins, the state variables are typically set to zero and the left side of equation 4 is non-zero. We can write an error vector

$$\mathbf{E}_k(\mathbf{X}) = \mathbf{Y}_k \mathbf{V}_k(\mathbf{X}) + \mathbf{I}_k(\mathbf{X}) + \mathbf{J}_k \quad (5)$$

whose Euclidean norm  $\mathbf{E}^T \mathbf{E} = \|\mathbf{E}\|$  is called the Harmonic Balance Error (HBE). If the HBE is reduced below a tolerance, we say that equation (4) is satisfied and a solution has been obtained.

- **Solving Methods**

The process of solving the harmonic balance equations is an iterative one. An estimate of  $\mathbf{X}$  is inserted into eqn. (5),  $\mathbf{E}$  is calculated and if it is not below the tolerance then a new value of  $\mathbf{X}$  must be determined and tried. Each such loop is termed

‘iteration’. There have been several methods used in the past to determine new values of  $\mathbf{X}$  and two that have proven to be the most general and efficient are discussed here.

The state variables  $\mathbf{X}$ , and harmonic balance residuals,  $\mathbf{E}$  are complex valued. In practice these are decomposed into their real and imaginary parts so that the number of real unknowns in  $\mathbf{X}$  is  $ND^*(2*Nt+1)$  where  $ND$  is the total number of nonlinear device ports and  $Nt$  is the number of frequency components ( $=NH$  for single tone analysis). Now we can write  $\mathbf{E}(\mathbf{X})=\mathbf{0}$  as a Taylor series expansion truncated after the first derivative term:

$$\mathbf{E}(\mathbf{X}) = 0 \approx \mathbf{E}(\mathbf{X}^{(n)}) + \mathbf{J}(\mathbf{X}^{(n)}) (\mathbf{X} - \mathbf{X}^{(n)}) \quad (6)$$

where  $\mathbf{J}$ , the Jacobian matrix, is the first derivative matrix of  $\mathbf{E}$  with respect to  $\mathbf{X}$  and superscript ‘n’ indicates the current iteration. Solving for  $\mathbf{X}$  and using this for the next trial:

$$\mathbf{X}^{(n+1)} = \mathbf{X}^{(n)} - \mathbf{J}^{-1}(\mathbf{X}^{(n)}) \mathbf{E}(\mathbf{X}^{(n)}) \quad (7)$$

This is the Newton-Raphson update method where the last right-hand term is the update. This method works in one iteration, if the set of equations is linear, but will take an unknown number of iterations if nonlinear. Often the update is reduced by a factor called the Newton damping factor, so the method takes smaller steps for each of the next iteration. Convergence to a solution is not guaranteed and the results of the iterations may diverge if not controlled. Harmonica uses enhanced versions of the Newton-Raphson method to improve convergence and speed.

Harmonica contains an algorithm that dynamically changes the Newton damping factor during solving, based on the rate of convergence. If the solver has trouble converging, the factor will be made smaller to improve convergence. If it has been reduced by more than a predetermined factor, the solver will stop and an error will be reported.

An important aspect to note is the size of the Jacobian. If  $\mathbf{X}$  contains  $ND^*(2*Nt+1)$  elements, then  $\mathbf{J}$  contains this number squared. As a practical example, if  $ND=10$  (5 FETs) and  $Nt=4$ , then there are 8100 entries in  $\mathbf{J}$  which takes 63 kBytes. This is relatively small, but  $Nt$  becomes much larger when multi-tone excitation is considered.

- **HBE tolerance**

### **HB<sub>TOL</sub> $x$**

Here  $x$  is the tolerance per device port per frequency component. The absolute harmonic balance error allowed is scaled by the number of device ports and number of frequency components so that large circuits with many frequency components meet similar HBE criteria as small circuits. The default for HB<sub>TOL</sub> is  $1.0 \times 10^{-6}$ . For the case of 2-tone intermodulation analysis and 3-tone analysis, the allowed harmonic balance is also scaled by the relative currents of the circuit. This reduces the allowed error (effectively reducing HB<sub>TOL</sub>) to provide better accuracy of the intermodulation products.

- **Multi-tone Analysis**

The discussion above was based on single-tone analysis for conceptual simplicity. Multi-tone analysis is simply an extension of single-tone [3]-[5]. In the single-tone case, a circuit is excited with an RF source and harmonics of that source are produced by the nonlinearities of the circuit. The set of harmonics, the frequency of excitation and DC are called the *spectrum* of the analysis. The single-tone spectrum is defined as:

$$S_1 = k * f_0 \\ k=0, 1, \dots, NH \quad (8)$$

where,  $f_0$  is the fundamental frequency. In multi-tone analysis the spectrum is modified to include the harmonic products of each fundamental tone. The harmonic products are just integer functions of the fundamental frequencies and indicate the allowed ‘bins’ for power conversion within a circuit. The rest of the harmonic balance analysis is exactly the same.

The conversion between time-domain waveforms and Fourier coefficients is accomplished by the discrete Fourier transform in single-tone analysis. For each additional fundamental tone, a dimension is added in the transform. This allows efficient computation between domains, but becomes CPU-intensive when more than three-dimensions are encountered.

### **Two-Tone Intermodulation Case**

The two-tone analysis spectrum is defined as:  $S_2 = |p * f_1 + q * f_2|$

$$|p|=0, 1, \dots, m1 \quad |q|=0, 1, \dots, m2 \quad (9)$$

where  $f_1$  and  $f_2$  are the first and second fundamentals, and  $m_1$  and  $m_2$  define the bounds of the spectrum. When the powers of the fundamentals are of similar magnitude, the bounds are chosen such that the harmonics and intermodulation products can be accurately assessed. The bounds are chosen as:

$$\begin{aligned} m_1 &= m_2 = M \\ |p| + |q| &\leq M \end{aligned} \quad (10)$$

$M$  is called the intermodulation order since it determines the order of intermodulation products that will be included in the spectrum. This selection results in a spectrum as shown in Figure 5, for  $M=3$ . The intermodulation products and harmonics are clearly seen. The total number of spectral components for this selection algorithm is

$$N_t = M * (M + 1) \quad (11)$$

### Two-Tone Mixer Case

When the power contained in one of the fundamentals is much greater than the other, as in a mixer case, then a spectrum is selected such that the harmonics of the strong signal (LO) and the sidebands of the LO and weak signal (RF) can be assessed. The bounds are then chosen as:

$$\begin{aligned} m_1 &= M_1 & m_2 &= M_2 \\ 0 \leq |p| \leq M_1 & \text{and} & 0 \leq |q| \leq M_2 \end{aligned} \quad (12)$$

Where,  $M_1$  is the number of LO harmonics and  $M_2$  is the number of sidebands on each side of the LO. This selection results in a spectrum as shown in Figure 5 for  $M_1=4$ ,  $M_2=2$ . The LO harmonics, sidebands and difference frequency are clearly seen. The total number of spectral components for this selection algorithm is

$$N_t = M_1 * (2 * M_2 + 1) + M_2 \quad (13)$$

### Three-Tone Intermodulation Case

The three-tone analysis spectra are very similar to two-tone and are defined by:  $S_3 = |p*f_1 + q*f_2 + r*f_3|$

$$|p|=0, \dots, m_1 \quad |q|=0, \dots, m_2 \quad |r|=0, \dots, m_3 \quad (14)$$

where  $f_3$  is the frequency of the third fundamental tone. The spectrum for the intermodulation case, where the power in the three tones is of the same order, and is

$$\begin{aligned} m_1 &= m_2 = m_3 = M \\ 0 \leq |p| + |q| + |r| &\leq M \end{aligned} \quad (15)$$

This selection results in a spectrum as shown in Figure 6, for  $M=3$ . Notice the much larger number of tones in the spectrum as compared with the two-tone case for  $M=3$ . The total number of spectral components is given by:

$$N_t = \frac{1}{3} * M * (M + 1) * (2M + 1) + 1 \quad (16)$$

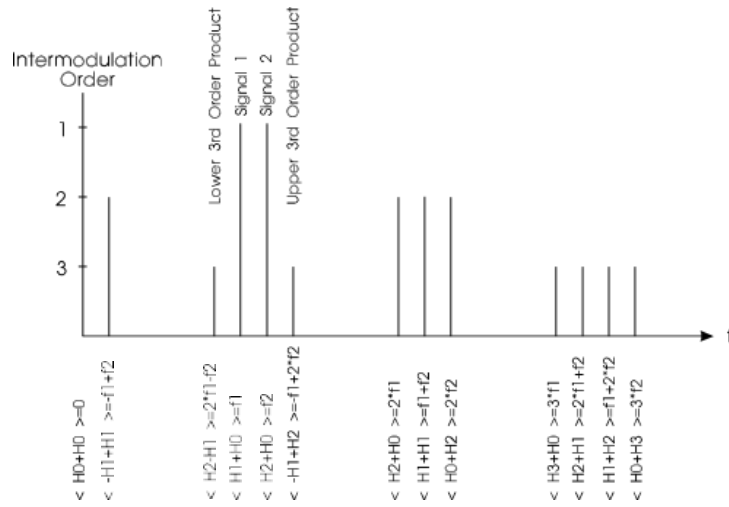


Figure 5: Two-tone intermodulation spectrum for  $M=3$

The vertical axis shows the intermodulation order for each spectral component.

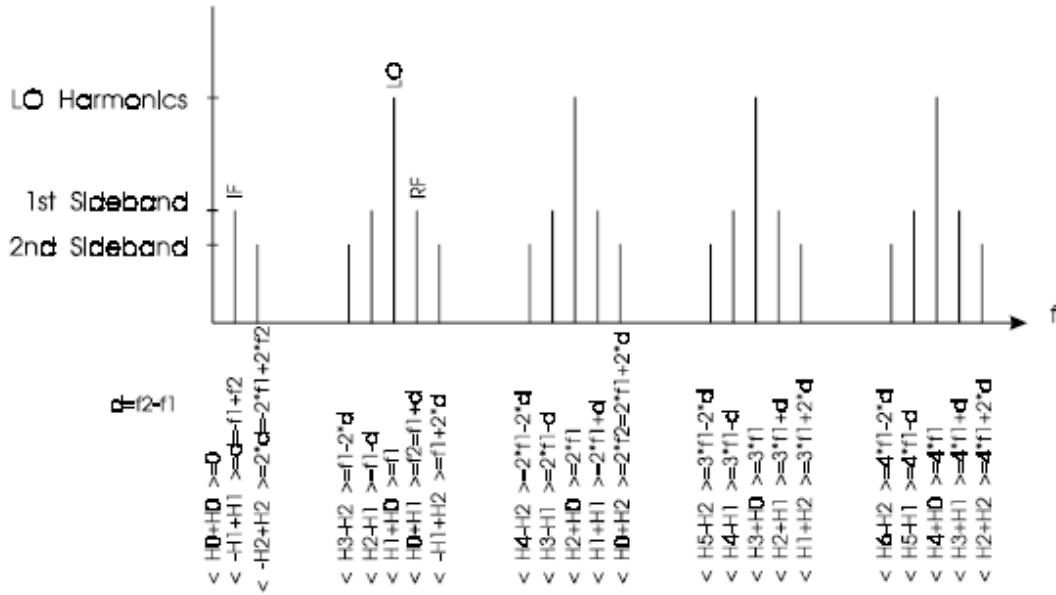


Figure 6: Two-tone spectrum for  $M1=4, M2=2$  (The vertical axis delineates the LO harmonics and sideband products)

### Three-Tone Mixer Case

For the mixer case, the spectrum is chosen assuming that one LO and two RF signals are present. The spectrum is selected by recognizing the intermodulation products of the RF signals as the quantities of interest. The intermodulation spectrum of the two isolated RF signals is then repeated on each side of the LO harmonics to form the three-tone mixer spectrum. This is given by:

$$m_1 = M_1 \quad m_2 = m_3 = M_2$$

$$0 \leq |p + q + r| \leq M_1 \quad 0 \leq |q| + |r| \leq M_2 \quad (17)$$

where  $M_1$  is the number of LO harmonics and  $M_2$  is the intermodulation order of the RF tones. The spectrum is shown in Figure 8 for  $M_1=2$  and  $M_2=3$ . The total number of spectral components is given by

$$N_t = M_1 * (2 * M_2^2 + 2 * M_2 + 1) + M_2^2 + M_2 \quad (18)$$

Generally, the number of frequency components required for three-tone analysis grows much faster than for two-tone analysis. This restricts the nonlinearity that can be computed. If four or more tones were considered, the number of frequency components becomes prohibitive unless smaller selection schemes are used.

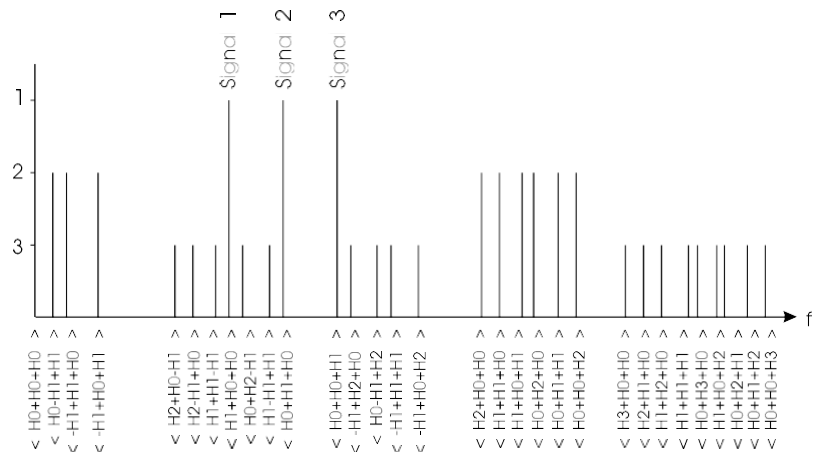
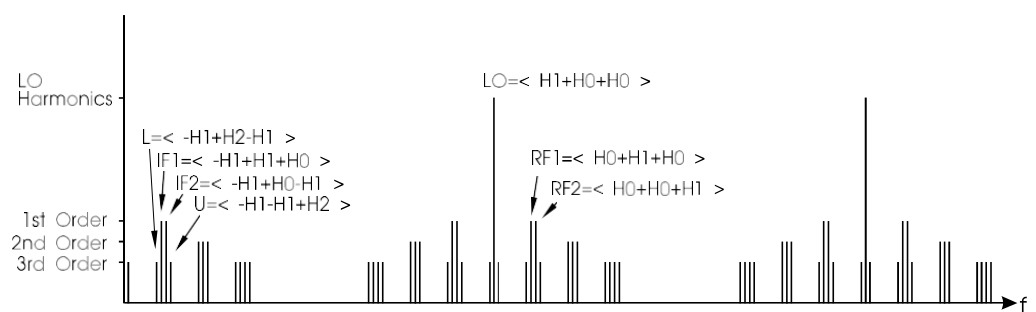


Figure 7: Three tone intermodulation spectrum for  $M=3$

The vertical axis shows the intermodulation order for each spectral component. Note that the products will change position depending on the separation between the fundamental tones. Here the difference between signal 3 and signal 2 is slightly greater than the difference between signal 2 and signal 1.



**Figure 8: Three tone mixer spectrum for M1=2, M2=3**

The intermodulation products of the two RF signals are shown to third order. Important spectral components are labeled.

- **Local Oscillator Spectrum Initialization of Mixer Circuits**

For mixer analysis cases where the primary interest is the conversion gain and the RF signal powers are small compared to the LO, the circuit can be analyzed using the LO signal only and the conversion gain is determined using small-signal (linear) frequency-conversion methods.

This is performed using the Small-Signal Mixer Analysis option (see the next section in this chapter).

For cases where the RF signal power is not insignificant compared to the LO, a full mixer spectrum must be used. Compression of the conversion gain due to high RF powers can then be analyzed. Here, the mixer problem can be divided into two parts to help speed the analysis.

Firstly, the LO signal is analyzed using single-tone analysis; the RF signal is turned off. Single-tone analysis is usually very fast compared with a full two-tone analysis. Once the LO signal spectrum is found, the results are used to initialize the full mixer spectrum and the RF signal is turned back on. The full spectrum is then analyzed.

This method is most useful for three-tone mixer problems, due to the large number of spectral components used in the analysis. The primary use of the three-tone mixer analysis is to determine the intermodulation products of the IF products. This precludes the use of small- signal mixer analysis (since the intermodulation products cannot be determined using linear frequency conversion methods), but the RF signals are generally small compared to the LO. By solving the LO problem first, which is the primary nonlinear problem, and then introducing the RF signals, the analysis time can be reduced by a factor of about three. The actual time reduction depends on the circuit, the RF power levels, and the conversion gain.

### Sparse Jacobian Techniques

The Jacobian matrix, when properly arranged, can be treated as a sparse matrix by pre-setting some entries to zero [6]. The physical reason for doing this is that most of the power transfer takes place between the harmonic frequencies of the fundamentals and much less takes place between the other frequencies in the spectrum. We can therefore set these derivatives to zero within the Jacobian. When this criterion is not met, the band of non-zero entries is widened to include cross-harmonic terms.

Because the Jacobian structure is properly arranged, sparse matrix techniques are efficiently employed. General purpose sparse matrix (Figure 9: Sparse Jacobian block structure) solvers that analyze the sparsity structure are avoided and specialized solvers can be used that are much more efficient. Harmonica automatically sets the bandwidth of the sparse tridiagonal matrix and dynamically alters it if the nonlinearity of the circuit is too great for the sparse assumptions. In this way the simulator achieves convergence using the minimal amount of computation time and memory that is possible for a given problem. For circuits with many devices under multi-tone operation, the CPU time may be decreased by a factor of 40.

The sparsity parameter will be dynamically altered during execution if needed. If  $n$  is greater than  $Nt/3$  ( $Nt$  is the number of frequencies), then the program will use the full Jacobian. If only the full Jacobian is desired, then set  $n$  to a large number.

**NOTE** Using a sparse Jacobian does not affect the final values or accuracy of the results. It will only affect the convergence properties of the particular problem.

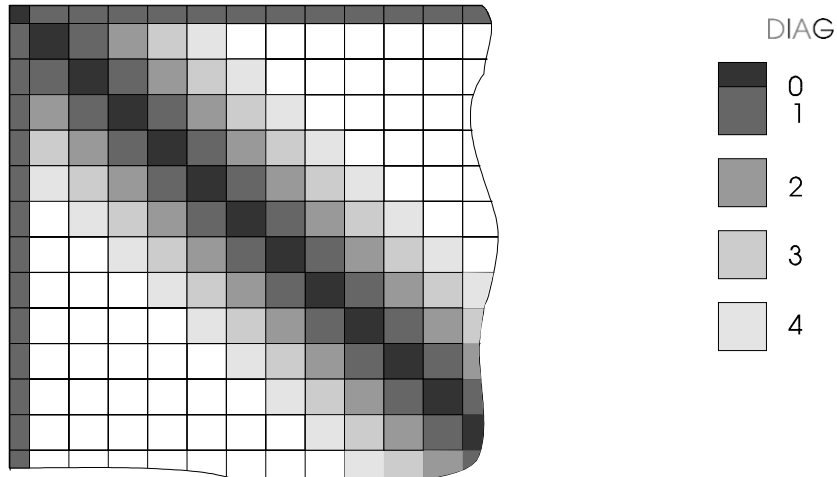


**Figure 9: Sparse Jacobian block structure**

### Iterative Newton Method

One of the short comings of harmonic-balance methods is the large memory requirements when a circuit has many nonlinear devices and/or multi-tone analysis is needed. The Jacobian system matrix grows large and must be stored and factored. Sparse methods may not be enough to keep the problem within the memory bounds and acceptable computational resources of desktop computers. Harmonica uses a technique that efficiently solves large systems of equations without direct factorization of the system matrix. In this way, there is no simplification or approximation made to the problem and the full accuracy of the conventional harmonic-balance method is completely maintained. The convergence and power-handling capabilities of conventional harmonic-balance analysis are also fully maintained. The method is completely automatic and does not require any user intervention. An internal software switch detects when the new method should be used and automatically invokes it.

A brief summary of the method and its advantages is given: Conventional harmonic-balance computes and stores the Jacobian matrix. The iterative solution of the harmonic-balance equations requires factorization of the Jacobian to obtain updates of the circuit voltages. As the number of nonlinear devices in the circuit increases and the number of spectral components used to analyze the circuit increases, the Jacobian matrix can become very large, requiring tens or hundreds of megabytes of storage and several minutes of CPU time to factor it. The calculation and factorization of the Jacobian typically occurs several times during a single harmonic-balance solution. The new methods, based on an iterative approach, known as *Krylov Subspace Methods*, avoid direct storage and factorization of the Jacobian. Rather, a series of matrix-vector operations replaces the full storage and factorization steps while retaining full numerical accuracy.

Observed speed-up factors depend on the number of nonlinear devices in the circuit and the number of spectral components used in the analysis as well as the convergence properties of the harmonic-balance algorithm. Speed improvements over conventional harmonic balance analysis from 2x to 10x for circuits consisting of a few transistors under two and three-tone excitation have routinely been observed. A circuit containing 20 FETs under three-tone analysis exhibited a speed improvement factor of 30x. Memory requirements have also been tremendously reduced. The 20 FET circuit originally required >200MB and now will analyze with 64MB. As the circuit becomes more “complex” the new methods provides better speed and memory improvements.

#### • **Generating Large-Signal S-Parameters**

The calculation of S-parameters in the large-signal regime is not as straightforward as it is in the linear, small-signal regime. The “large-signal S-parameters”, are dependent on the power of the excitation sources at each external circuit port as well as the circuit bias and terminations.

Guidelines will be given here on using Harmonica to generate large-signal S-parameters, but the proper use of these S-parameters in circuit design is up to you.

Consider a two-port circuit whose large-signal S-parameters are desired. If we apply a source at port 1 with port 2 terminated, we could measure the reflected and transmitted waves, and conversely for a source applied to port 2 [7]. However, this assumes that when the device under test is actually used, it will be terminated in the same impedance as it was tested. This is rarely the case. Typically the device is embedded in some matching network which presents complex impedance to the device. Therefore, the operating regime of the device will change and its large-signal S-parameters will be altered.

We could then hypothesize that a source can be placed at each port and the travelling waves could be measured at each port. The problem here is that it is not possible to distinguish between the reflected wave at a port and the transmitted wave due to the source at the other port because the sources are the same frequency. If we perturb the frequency of one of the sources, then the reflected and transmitted waves due to each source can be resolved. This, however, requires a two-tone analysis. The situation is illustrated in Figure 10 (a, b, c) for the two-port device under test.

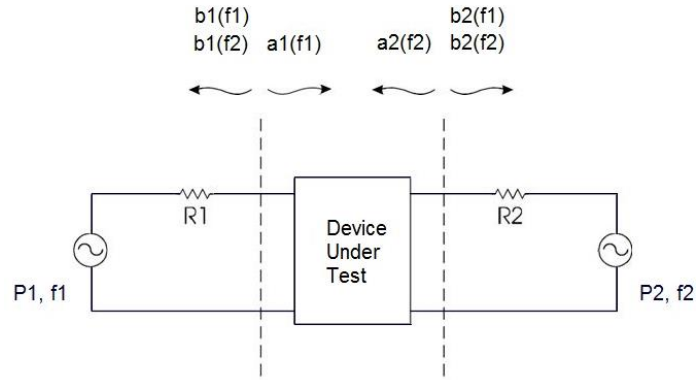


Figure 10 (a) Test setup for determining two-port one-port and three-port large-signal S-parameters.

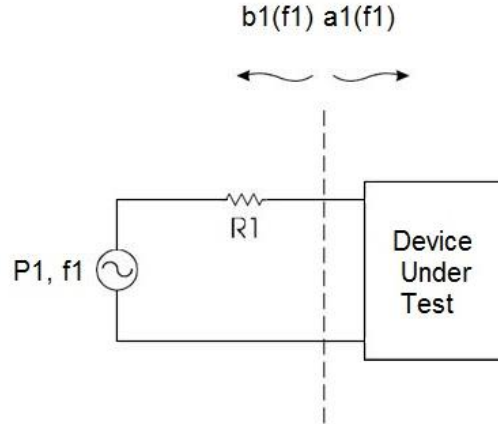


Figure 10 (b) Test setup for determining two-port one-port and three-port large-signal S-parameters.

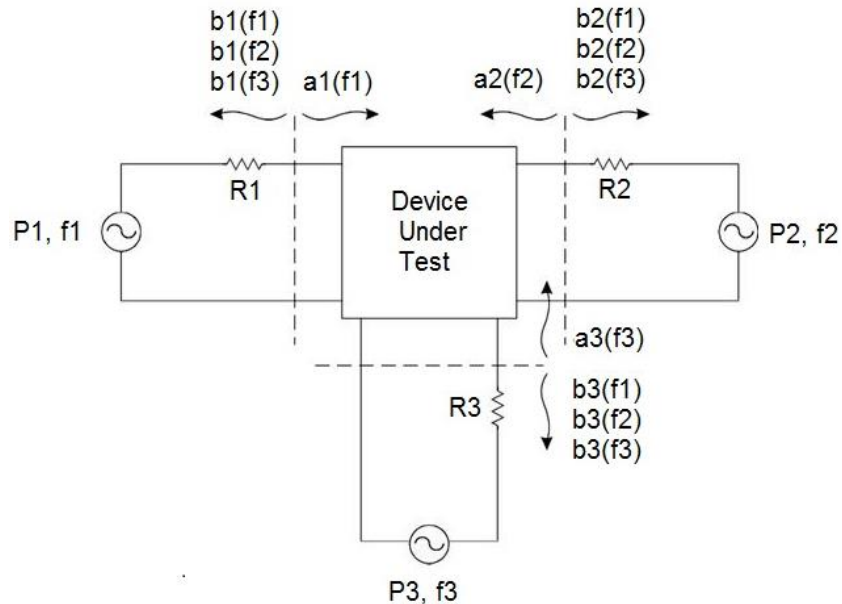


Figure 10 (c) Test setup for determining two-port one-port and three-port large-signal S-parameters

The difference in frequency between the two sources can be made small, on the order of 0.001%. This is recommended for circuits of large Q. Typically the difference used is about 0.1% because the S-parameters of the device under test do not change rapidly with frequency. To measure the travelling waves, we use the return loss and transducer gain output responses in the **nout** block.

- *Nonlinear Noise Analysis*

## Overview

Noise performance of microwave circuits is one of the major concerns for circuit design engineers. It is an important determining factor of receiver system sensitivity and dynamic range. Linear simulators are ideal to predict the noise performance of circuits using arbitrary combinations of active and passive elements. However most microwave circuits need be analyzed using nonlinear analysis techniques since the applied signals may cause the circuit to operate closely to a saturated mode and result in nonlinear operation. This section illustrates how the noise performance of general mixer or multiplier/divider circuits is simulated by using the techniques implemented in Harmonica.

The goal of the noise analysis is to find the spectral distribution of the noise power actually delivered to the load. Three different noise analysis capabilities have been implemented:

- For Mixer Noise Analysis, the noise figure from the RF signal input to the IF load can be determined [14][17]
- For single-tone circuits with a large-signal input, such as a frequency multiplier or divider, the noise analysis can determine the noise power spectral distribution and amplitude and phase noise near a specified harmonic [15] [16]
- For oscillator circuits, the phase and amplitude noise power delivered to a load can be determined.

The first two topics are discussed in this section. For a discussion on oscillator noise analysis, please refer to the *Oscillator Analysis* chapter in this volume.

## Basic Information about Noise Calculations

A circuit biased at DC without RF excitation generates noise due to thermal noise and the bias current in the active devices (flicker noise and shot noise). The noise is dependent on the bias point of the active devices and is uncorrelated. When the device is pumped by an RF excitation (e.g. the LO), the nonlinear noise sidebands are modulated and are partially correlated because each sideband is a combination of the original uncorrelated DC sidebands. That is, the excitation modulates the instantaneous operating point of the device and due to the device nonlinearity, the noise sidebands are converted in frequency to other harmonic sidebands.

During the frequency conversion, each sideband generates correlated components in the vicinity of the IF (or any other spectral frequency). Noise figure can be determined from these noise components which are dissipated in the IF load. In addition, contributions to the noise power at the IF load are also made by both the noise injected by the LO source and the thermal noise generated by the linear network. Because they are uncorrelated, their noise power contributions are additive. Figure 11 illustrates the general concept of the noise calculation.

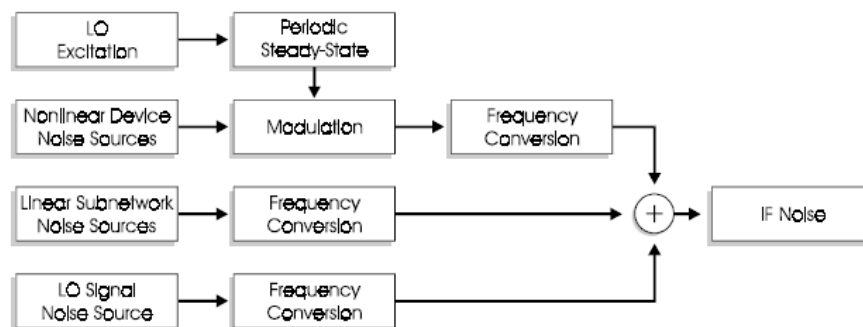


**Figure 11:** IF noise in a general nonlinear mixer circuit

Figure 11 can be viewed in three pieces. The nonlinear devices are modulated by the LO (or other source), and the noise due to the devices are contributed to the IF load through frequency conversion. The second piece is the noise from the linear subnetwork, which, through frequency conversion, makes it to the IF load. Finally, noise present in the LO can make it to the

IF load through frequency conversion. The summation of noise powers indicates that noise from the three sources is uncorrelated.

In the following, various noise sources considered in the noise analysis of nonlinear circuits are described.

- **Thermal Noise Sources in a Passive Subnetwork**

In a linear passive network, noise arises only from the losses in the network. The noise correlation matrix for a linear passive subnetwork is directly related to losses represented in the admittance matrix:

$$C_n = 2K_B T d_f (Y + Y^*) \quad (20)$$

where  $Y$  is the admittance matrix of the passive network; “\*” indicates the conjugate transpose;  $K_B$  is Boltzmann's constant;  $T$  is the ambient temperature, and  $d_f$  is the noise bandwidth. The linear analysis of the circuit automatically computes the noise matrix. No special keywords are required.

- **Noise Models of Active Devices**

The noise models of the active devices vary from device to device. All have a shot noise component which is proportional to the instantaneous current through the active region of the device. The models also have a flicker noise (1/f) component which is important for low frequency mixer IF and near-carrier noise in oscillators.

- **Statistical Noise of an Exciting Source**

The specification of the noise associated with the excitation is shown graphically in Figure 12.  $FDEV_i$  is the frequency deviation of the  $i$ 'th noise sideband.  $RFUP_i$  is normalized upper sideband of the  $i$ 'th noise power component in units of dBc/Hz

It is specified in decibels relative to the carrier (LO in the figure). Likewise,  $RFLO_i$  is the normalized lower sideband. For a complete statistical description, the correlation between the upper and lower sidebands can also be specified.

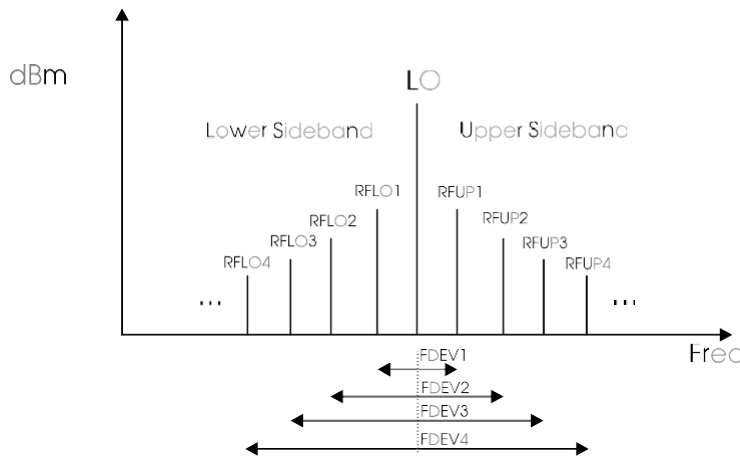


Figure 12:  $FDEV_i$  is the frequency deviation of the  $i$ 'th noise sideband

The mean-square value of the amplitude fluctuations (normalized amplitude noise) is given from the upper and lower complex phasors of the noise components in a 1Hz band located at the lower and  $R$  upper sidebands:

$$\langle |\delta A|^2(f_d) \rangle = 2 \frac{\langle |V_1(f_d)|^2 \rangle + \langle |V_u(f_d)|^2 \rangle + 2Re[\langle V_1^*(f_d)V_u^*(f_d) \rangle \exp(2j\Phi_0)]}{|V_0|^2} \quad (21)$$

The mean-square value of the phase fluctuations (normalized phase noise) in a 1Hz band at a frequency deviation  $f_d$  from the carrier (PM noise) is given by:

$$\langle |\delta \Phi|^2(f_d) \rangle = 2 \frac{\langle |V_1(f_d)|^2 \rangle + \langle |V_u(f_d)|^2 \rangle - 2Re[\langle V_1^*(f_d)V_u^*(f_d) \rangle \exp(2j\Phi_0)]}{|V_0|^2} \quad (22)$$

A complete statistical description of the noisy source requires that the two real quantities

$\langle V_1(f_d) V_1^*(f_d) \rangle$ ,  $\langle V_u(f_d) V_u^*(f_d) \rangle$  and the complex quantity  $\langle V_1^*(f_d) V_u^*(f_d) \rangle$  be assigned as a function of the frequency deviation from the carrier. However, in many practical cases, a full statistical description of the noisy source is not available, because the information on the sourcenoise is produced by measurements which only provide the R.F. spectrum and the AM noise (orequivalently the FM and AM noise). In this case, one of the alternatives of the reduced data setcan be used.

It is worth noting that in practice the normalized amplitude noise is often several tens of dBs lower than the phase noise (or, equivalently, than the R.F. spectrum), especially at low frequencydeviations. In such cases the noise analysis may become ill-conditioned from the viewpoint of numerical accuracy. Relatively large values of the numbers of sampling points may then be required to produce correct results.

- **Noise Figure and Noise Spectrum Calculations**

A mixer noise figure calculation determines the noise added by the circuit under investigationrelative to the noise injected into the circuit by the source. It is given by:

$$NF = \frac{SNR_{in}^{RF}}{SNR_{out}^{IF}} = \frac{N_{out}^{IF}}{N_{in}^{RF}} \frac{1}{G_c} \quad (23)$$

where,  $N^f$  is the noise power at port  $p$ , frequency  $fG_C$  is the conversion gain of the mixer

Within the simulation, the RF source and LO source are considered noisy and the IF termination is considered noiseless. These sources contribute noise at all frequencies and the double-sideband (DSB) noise figure is calculated.

The calculation of noise spectrum for single-tone analysis (including amplifiers, oscillators, multipliers, etc.) determines the noise power relative to the specified harmonic, the absolute noise power absorbed by the load at the specified harmonic is computed and normalized (in dBc) to that harmonic power. In this case,both the source termination and the load termination are considered noisy.

## References

- [1] V. Rizzoli, A. Lipparini, and Ernesto Marazzi, "A General-Purpose Program for Nonlinear Microwave Circuit Design," *IEEE Trans. Microwave Theory Tech.*, vol. 31,no. 9, pp. 762-770, September 1983.
- [2] V. Rizzoli, A. Lipparini, A. Costanzo, F. Mastri, C. Cecchetti, A. Neri, and D. Masotti,"State-of-the-Art Harmonic-Balance Simulation of Forced Nonlinear Microwave Circuits by the Piecewise Technique," *IEEE Trans. Microwave Theory Tech.*, vol. 40, no. 1, pp. 12-28, January 1992.
- [3] V. Rizzoli, C. Cecchetti, A. Lipparini, " A General-Purpose Program for the Analysisof Nonlinear Microwave Circuits Under Multitone Excitation by Multidimensional Fourier Transform," *17th European Microwave Conf.*, pp. 635-640, September 1987.
- [4] V. Rizzoli and A. Neri, "State-of-the-Art and Present Trends in Nonlinear Microwave CAD Techniques," *IEEE Trans. Microwave Theory Tech.*, vol. 36, no. 2, pp. 343-365,February 1988.
- [5] V. Rizzoli, C. Cecchetti, A. Lipparini, and F. Mastri, "General-Purpose Harmonic- Balance Analysis of Nonlinear Microwave Circuits Under Multitone Excitation," *IEEE Trans. Microwave Theory Tech.*, vol. 36, no. 12, pp. 1650-1660, December 1988.
- [6] V. Rizzoli, F. Mastri, F. Sgallari, V. Frontini, "The Exploitation of Sparse-Matrix Techniques in Conjunction with the Piecewise Harmonic-Balance Method for Nonlinear Microwave Circuit Analysis," *1990 MTT-S Int. Microwave Symp. Digest*,pp. 1295-1298, June 1990.
- [7] V. Rizzoli, A. Lipparini, and F. Mastri, "Computation of Large-Signal S-Parameters by Harmonic-Balance Techniques," *Electron. Lett.*, vol. 24, pp. 329-330, Mar. 1988.
- [8] V. Rizzoli, F. Mastri, and F. Sgallari, and G. Spaletta, "Harmonic-Balance Simulationof Strongly Nonlinear Very Large-Size Microwave Circuits by Inexact Newton Methods," *IEEE MTT-S*, pp. 1357-1360, 1996.
- [9] George D. Vendelin and Anthony M. Pavio, U. L. Rohde, "Microwave circuit design using linear and nonlinear techniques", Wiley, New York, 2005

- [10] V. Rizzoli, A. Neri, and A. Costanzo, "Analysis and Optimization of DROs Using a General Purpose CAD Program," *Alta Frequenza*, Vol. 57, September 1988, pp. 389–398.
- [11] A. Neri and V. Rizzoli, "Global Stability Analysis of Microwave Circuits by a Frequency-Domain Approach," *IEEE MTT-S International Microwave Symposium Digest*, June 1987, pp. 689–692.
- [12] H. Wacker, *Continuation Methods*, Academic Press, New York, 1978.
- [13] G. Ioos and D. D. Joseph, *Elementary Stability and Bifurcation Theory*, Springer-Verlag, New York, 1980.
- [14] V. Rizzoli, F. Mastri, and C. Cecchetti, "Computer-Aided Noise Analysis of MESFET and HEMT Mixers," *IEEE Trans. Microwave Theory Tech.*, vol. 37, no. 9, pp. 1401–1410, September 1989.
- [15] V. Rizzoli, F. Mastri, and D. Masotti, "General-Purpose Noise Analysis of Forced Nonlinear Microwave Circuits," *1992 Military Microwaves*, pp. 293–298, 1992.
- [16] V. Rizzoli, F. Mastri, and D. Masotti, "Advanced Piecewise-Harmonic-Balance Noise Analysis of Nonlinear Microwave Circuits with Applications to Schottky-Barrier Diodes," *1992 MTT-S Int. Microwave Symp. Digest*, pp. 247–250, June 1992.
- [17] C. R. Chang, and J. Gerber, "Nonlinear Noise Analysis for Wireless Communication Systems," *1993 RF Expo West*, pp. 254–260, March 1993.

### Interesting Reads

1. Ulrich L. Rohde, "Designing A Matched Low Noise Amplifier Using CAD Tools," *Microwave Journal*, Oct. 1986.
2. U. L. Rohde, "All about Phase Noise in Oscillators," *QEX*, Dec. 1993, Jan. 1994, Feb. 1994
3. Ulrich L. Rohde and Chao-Ren Chang, "The Accurate Simulation of Oscillator and PLL Phase Noise in RF Sources," *Wireless '94 Symposium*, Santa Clara.
4. Ulrich L. Rohde, Chao-Ren Chang, and Jason Gerber, "Design and Optimization of Low-Noise Oscillators using Nonlinear CAD Tools," presented at the Frequency Control Symposium, Boston, MA June 1-2, 1994.
5. U. L. Rohde, "Designing and Optimizing Low Phase Noise Oscillators using Harmonic Balance Simulators and Advanced Parameter Extraction," Session B3-3, 2nd IEEE Joint Chapter Workshop I conjunction with CAE, Modeling and Measurement Verification, October 24, 1994, Wembley Conference Centre, London, UK.
6. Ulrich L. Rohde and Chao-Ren Chang, "Analysis and Optimization of Oscillators for Low Phase Noise and Low Power Consumption," *RF Design*, pp70-79, March, 1995.
7. U. L. Rohde, "Designing SAW and DRO Oscillators Using Nonlinear CAD Tools," 1995 IEEE International Frequency Control Symposium, San Francisco, CA, May 30, 1995 – June 2, 1995.
8. U.L. Rohde, "Now nonlinear Noise Model for MESFETs including MM-Wave Application," First International Workshop of the West German IEEE MTT/AP Joint Chapter on Integrated Nonlinear Microwave and Millimeter Circuits (INMMC'90) Digest, October 3-5, 1990, Duisburg University, Duisburg, West Germany.
9. R.A. Pucel, W. Struble, R. Hallgren, and U. L. Rohde, "A General Noise De-embedding Procedure for Packaged Two-Port Linear Active Devices," *IEEE Transactions on Microwave theory and Techniques*, Vol. 40, No. 11. pp. 2013-2024, November 1992.
10. U. L. Rohde and C.R. Chang, "Parameter Extraction for Large Signal Noise Models and Simulation of Noise in Large Signal Circuits like Mixers," *Microwave Journal*, pp222-239, May, 1993.
11. R. A. Pucel and U.L. Rohde, "An Accurate Expression for the Noise Resistance Rn of a Bipolar Transistor for Use with the Hawkins Noise Model," *IEEE Microwave and Guided Wave Letters*, Vol. 3, No. 2, pp. 35-37, February, 1993.
12. U. L. Rohde, "Parameter Extraction for Large Signal Noise Models and Simulation of Noise in Large Signal Circuits Like Mixers and Oscillators," 23rd European Microwave Conference, Madrid, Spain, September 6-9, 1993
13. Ulrich L. Rohde, Anthony M. Pavio, and Robert A. Pucel, "Accurate Noise Simulation of Microwave Amplifiers Using CAD", *Microwave J*, 31(12), 130-141, December 1988.

14. George D. Vendelin Anthony M. Pavio, Ulrich L. Rohde, Matthias Rudolph, *Microwave Circuit Design Using Linear and Nonlinear Techniques*, 3rd Edition, John Wiley: ISBN: 978-1-119-74170-1 April 2021 *Microwave and Wireless Synthesizers: Theory and Design*, 2nd Edition
15. Ulrich L. Rohde, Enrico Rubiola, Jerry C. Whitaker, *Microwave and Wireless Synthesizers: Theory and Design*, 2nd Edition , John Wiley, ISBN: 978-1-119-66600-4 April 2021
16. Ulrich L. Rohde, Matthias Rudolph, *RF / Microwave Circuit Design for Wireless Applications*, 2nd Edition, John Wiley, ISBN: 978-1-118-43148-1 January 2013

#### **Additional References**

1. Ulrich L. Rohde and T. T. N. Bucher, *Communications Receivers: Principles & Design* (New York: McGraw-Hill Book Company, 1987).
2. George Vendelin, Anthony M. Pavio and Ulrich L. Rohde, *Microwave Circuit Design Using Linear and Nonlinear Techniques* (New York: John Wiley & Sons, January 1990).
3. R. Bhatia, J. Gerber, and T. Kwan, “Analyze Large-Signal Distributed Amps with Nonlinear CAE,” *Microwaves and RF*, November 1989, pp. 121-129.
4. Ulrich L. Rohde, Anthony M. Pavio, and Robert A. Pucel, “Accurate Noise Simulation of Microwave Amplifiers Using CAD,” *Microwave Journal*, December 1988.
5. “All About Phase Noise in Oscillators,” *QEX*, December 1993, January 1994, February 1994.
6. J. Gerber, L. Mah, C. R. Chang, M. Eron, and T. Kwan, “State-of-the-Art Nonlinear CAD for Microwave/RF Circuit Design,” *1991 RF Expo East Digest*, pp 1-29.
7. J. Gerber and R. Gilmore, “Nonlinear Microwave CAD Applications,” *1990 Workshop on Analog Circuit Engineering*, Raleigh, NC.
8. M. Eron, J. Gerber, L. Mah, and W. Tompkins, “MESFET Model Extraction and Verification Techniques for Nonlinear Applications,” *1990 Asia-Pacific Microwave Conference*, pp. 321-324.
9. R. A. Pucel, W. Struble, R. Hallgren and U. L. Rohde, “A General Noise De-embedding Procedure for Packaged Two-Port Linear Active Devices,” *IEEE Transactions on Microwave Theory and Techniques*, Vol. 40, No. 11, November 1992, pp. 2013-2024.

10. R. Pengelly, R. Tayrani, J. Gerber, and U. L. Rohde, "The Simulation of Temperature Effects in Small-Signal, Linear, and Large-Signal, Nonlinear Circuits," *1993 IEEE MTT-S Workshop on Thermal Aspects of Microwave Device and Circuit CAD*.
11. C. R. Chang, J. Gerber, and R. Pengelly, "Nonlinear Noise Analysis for Wireless Communication Systems," *1993 RF Expo West Digest*, pp 254-260.
12. "New Nonlinear Noise Model for MESFETS Including MM-Wave Application," *First International Workshop of the West German IEEE MTT/AP Joint Chapter on Integrated Nonlinear Microwave and Millimeterwave Circuits (INMMC '90) Digest*, October 3-5, 1990, Duisburg University, Duisburg, West Germany.
13. "Improved Noise Modeling of GaAs FETS: Using an Enhanced Equivalent Circuit Technique," *Microwave Journal*, November 1991, pp. 87-101; December 1991, pp. 87-95.
14. U. L. Rohde and C. R. Chang, "Parameter Extraction for Large Signal Noise Models and Simulation of Noise in Large Signal Circuits Like Mixers," *Microwave Journal*, May 1993, pp. 222-239.
15. "Super-Compact Enhancement Will Predict Yield," *Microwaves & RF*, June 1987.
16. J. Gerber and R. Gilmore, "Active Device Parameter Extraction for Oscillator Simulation," *1989 WESCON Conference Record*, pp. 83-87.
17. "Parameter Extraction for Large Signal Noise Models and Simulation of Noise in Large Signal Circuits Like Mixers and Oscillators," *23rd European Microwave Conference*, Madrid, Spain, September 6-9, 1993.
18. "The Accurate Simulation of Oscillator and PLL Phase Noise in RF Sources," Chao-Ren Chang and U. L. Rohde, *Wireless '94 Symposium*, Santa Clara, California.
19. Ulrich L. Rohde, Chao-Ren Chang, and Jason Gerber, "Design and Optimization of Low-Noise Oscillators using Nonlinear CAD Tools," *Frequency Control Symposium*, Boston, Massachusetts, June 1-2, 1994.
20. "Designing SAW and DRO Oscillators Using Nonlinear CAD Tools," *1995 IEEE International Frequency Control Symposium*, San Francisco, California, May 30 to June 2, 1995.
21. Ulrich L. Rohde and Chao-Ren Chang, "Frequency Domain and Time Domain Analysis and Optimization of Oscillators for Low Phase Noise and Lower Power Consumption," *Communications Quarterly*, 1995.
22. *Design and Simulation of a Bipolar Gilbert-Cell Mixer* (Paterson: Compact Software, 1994; application note).
23. Q. Cai, J. Gerber, U. L. Rohde, and T. Daniel, "HBT High Frequency Modeling and Integrated Parameter Extraction," *IEEE Trans. on MTT*, vol. 45, no. 12, pp. 2493-2502, Dec. 1997.
24. J. Gerber and C. R. Chang, "Application of Harmonic-Balance Analysis to the Stability Analysis of Oscillators," *1997 IEEE MTT-S*, pp. 1587-1590, 1997.
25. Q. Cai, J. Gerber, T. Daniel, and U. L. Rohde, "Transistor Parameter Extraction Using DC, S-Parameter, and Noise Data Simultaneously," *1997 IEEE MTT-S*, pp. 861-864, 1997.
26. J. Gerber, C. R. Chang, and U. L. Rohde, "Harmonic-Balance Analysis and Optimization of Oscillator Properties Including Phase Noise," *1994 Asia-Pacific Microwave Conf.*, pp. 867-870